On the Etching Mechanism of Parylene-C in Inductively Coupled O_2 Plasma

D.A. Shutov
Department of Electronic Devices & Materials Technology, Ivanovo State University of Chemistry & Technology, 7 F. Engels st., 153000 Ivanovo, Russia

Sungihl Kim
Department of IT Electronics Engineering, Daejeon University, 96-3 Yongun-dong, Dong-gu, Daejeon 300-716, Korea

Kwang-Ho Kwon[a]
Department of Control and Instrumentation Engineering, Korea University, Jochiwon-eup, Yeongi-gun, Chungnam 339-700, Korea

[a]E-mail: kwonkh@korea.ac.kr

(Received June 16 2008, Accepted August 14 2008)

We report results on a study of inductively coupled plasma (ICP) etching of Parylene-C (poly-monochloro-para-xylylene) films using an O_2 gas. Effects of process parameters on etch rates were investigated and are discussed in this article from the standpoint of plasma parameter measurements, performed using a Langmuir probe and modeling calculation. Process parameters of interest include ICP source power and pressure. It was shown that major etching agent of polymer films was oxygen atoms $O(^3P)$. At the same time it was proposed that positive ions were not effective etchant, but ions played an important role as effective channel of energy transfer from plasma towards the polymer.

Keywords : Parylene-C, Oxygen plasma, Etching mechanism, Plasma modeling

1. INTRODUCTION

Parylene-C (poly-monochloro-para-xylylene) is used as a gate dielectric material in an organic field-effect transistor (OTFT)[1,2], due to its robustness as a dielectric film, its ability to form pinhole-free films, and its fabrication with vapor deposition method. The Parylene-C gate insulator also has low leakage current density and low energetic disorder at the semiconductor-insulator interface due to its low polarity.

One of the widely distributed processes in microelectronics industry is dry etching. A systematic investigation of the etch mechanism of microelectronic materials, particularly Parylene-C, is important. O_2 plasma is normally used for dry etching of polymers. However, Parylene-C etch rates in the ICP O_2 discharge over the wide range of the operating parameters are yet to be explored. Mechanisms of polymer etching are not clearly understood. In this work, the effects of the operating parameters like gas pressure, ICP source power, and bias power on the parylene-C etch rate in the O_2 ICP discharge have been investigated, to understand the etching mechanism for Parylene-C. Plasma diagnostics was performed by using a Langmuir probe. To establish the basic relationships between operating parameters and Parylene-C etch behavior, the simplified model of discharge was applied.

2. EXPERIMENTAL

2.1 Experimental setup

300-nm thick Parylene-C films were deposited on Si (100) substrates by chemical vapor deposition (CVD). The wafers were then plasma-treated using an radiofrequency (RF) ICP system. Etching experiments were performed by using a commercially available ICP system. The reactor consisted of a cylindrical quartz chamber with a radius (R) of 16 cm and a 5-turns copper coil located on a 10-mm-thick horizontal quartz window. The coil was connected to a 13.56 MHz power supply. The distance between the horizontal quartz window and

bottom anodized aluminum electrode used as a substrate holder (L) was 12.8 cm. The bottom electrode was connected to another 13.56 MHz power supply to produce a negative DC bias voltage.

In the current work, ICP source power varied from 200 to 500 W, bias power from 0 to 100 W, pressure from 4 to 10 mTorr, and O_2 total gas flow was kept constant at 60 cm^3/min.

To monitor the etch rate, the 2x2 cm^2 sized samples were used. The etched depth of the Parylene was measured using a surface profiler (Alpha-step 500, Tencor). The etch rate was calculated as "decreased thickness" divided by the exposure time.

Plasma diagnostics was represented by a double Langmuir probe (DLP2000, Plasmart Inc.). The probes were installed through the view-port on the side wall of the reactor chamber and centered in a radial direction. Plasma parameters (electron temperature, plasma potential, floating potential, and ion density) were calculated by the software (DLP2000) supplied by the equipment manufacturer.

The qualitative composition of gaseous reaction products was measured by a quadrupole HIDEN Hal 511 mass-spectrometer. For the mass spectrometer analysis, gas samples were extracted from the bottom of the vacuum chamber. Calibration of the signals on individual gases was not done.

2.2 Simplified volume-averaged model for O_2 plasma

To obtain data on the densities and fluxes of oxygen plasma active species, we used a simplified global (volume-averaged) model of plasma chemistry in high-density oxygen discharges developed by Lee *et. al.*[3,4] which has been verified and improved by others authors[5-8]. The model includes seven types of species, namely O_2, $O(^3P)$, $O(^1D)$, O_2^+, O^+, O^- and electrons. The list of processes taken into account by the model for oxygen discharge is specified in Table 1.

Volume-average density of charged species was calculated using the combination of the quasi-neutrality condition for bulk plasma with the kinetic equations for both negative and positive ions. The quasi-neutrality condition was written as $n_e + n_{O^-} = n_+$, where $n_+ = n_{O^+} + n_{O_2^+}$ is the total density of positive ions known from the Langmuir probe measurements. In the balance equation for negative ions $\left(k_9 n_{O^+} + k_{10} n_{O_2^+} + k_{11} n_e\right) n_{O^-} = k_3 n_e n_{O_2}$, we neglected the heterogeneous decay of O^- assuming the quasi-neutrality condition for the chamber wall to be written as $\Gamma_e \approx \Gamma_{O_2^+} + \Gamma_{O^+}$, where Γ is the flux of particles. The partial density of positive ions in their total density was calculated according to the following equations

$$\left(k_{10} n_{O^-} + k_{16}\right) n_{O_2^+} = k_1 n_e n_{O_2}$$
$$\left(k_9 n_{O^-} + k_{12} n_{O(^1D)} + k_{15}\right) n_{O^+} = k_6 n_e n_O$$

Effective rate coefficients of the heterogeneous decay for oxygen ions in Reaction 15 and 16 are estimated by the following expression:

$k = 2u_{B,(O^+,O_2^+)} \times (R^2 h_L + RLh_R)/R^2 L)$, where $u_{B,(O^-,O_2^+)}$ is the ion Bohm velocity that was calculated as

$u_{B,(O^+,O_2^+)} = \sqrt{eT_e(1+\alpha_s)/((1+\alpha_s T_e/T_i)m_i)}$.

Here $\alpha_s = \alpha[\exp((1+\alpha_s)(T_e/T_i - 1)/(2+2\alpha_s T_e/T_i))]^{-1}$ is the relative density of negative ions at the plasma sheath edge[3]. For simplicity, we assumed the temperature of all kinds of ions to be equal and dependent only on gas pressure which follows an empirical correlation from Refs.[4]: $T_i \approx T + (0.5 - T)/p$, where T is in "eV" and p is in "mTorr". The correction factors h_L and h_R for the radial and axial sheath sizes are given by the low pressure diffusion theory described in Refs. 4 and 9.

Volume-average density of neutral ground-state species in steady-state region was estimated using the balance equations of chemical kinetics written as follows:

$$n_{O_2} = n_0 \frac{T_0}{T} - 0.5 n_o$$
$$(k_2 + 2k_4) n_{O_2} n_e + (k_5 n_{O_2} + 2k_8 n_{O(^3P)} + k_{13}) n_{O(^1D)}$$
$$= (k_7 n_e + k_8 n_{O(^1D)} + k_{14} + \frac{1}{\tau_R}) n_{O(^3P)}$$
$$(k_2 n_{O_2} + k_7 n_{O(^3P)}) n_e$$
$$= (k_5 n_{O_2} + k_8 n_{O(^3P)} + k_{13} + \frac{1}{\tau_R}) n_{O(^1D)} ,$$

where k are the rate coefficients for the processes specified in Table 1 and τ_R is the residence time. The residence time was calculated as [3]: τ_R = *Vol / pumping speed*, where *Vol* is the volume of the system and the *pumping speed* is defined as operating pressure / flow rate. Although all three neutral species were pumped away at slightly different speeds due to the difference in mass, in this model, it was assumed the pumping loss for all three species were identical.

Table 1. Reaction set for O_2 plasma modeling.

Process		Rate coefficient	Reference
$O_2 + e \rightarrow O_2^+ + 2e$	R1	$2.34\times10^{-9} T_e^{1.03} \exp(-12.29/T_e)$	9
$O_2 + e \rightarrow O(^3P) + O(^1D) + e$	R2	$3.49\times10^{-8} \exp(-5.92/T_e)$	9
$O_2 + e \rightarrow O(^3P) + O^-$	R3	$1.07\times10^{-9} T_e^{-1.391} \exp(-6.26/T_e)$	9
$O_2 + e \rightarrow O(^3P) + O(^3P) + e$	R4	$6.86\times10^{-9} \exp(-6.29/T_e)$	9
$O_2 + O(^1D) \rightarrow O(^3P) + O_2$	R5	4.0×10^{-11}	4, 5
$O(^3P) + e \rightarrow O^+ + 2e$	R6	$9.00\times10^{-9} T_e^{0.7} \exp(-13.6/T_e)$	8
$O(^3P) + e \rightarrow O(^1D) + e$	R7	$4.54\times10^{-9} \exp(-2.36/T_e)$	8
$O(^3P) + O(^1D) \rightarrow O(^3P) + O(^3P)$	R8	8.1×10^{-12}	8
$O^+ + O^- \rightarrow O(^3P) + O(^3P)$	R9	$4.0\times10^{-8} (300/T)^{0.43}$	8
$O_2^+ + O^- \rightarrow O(^3P) + O_2$	R10	$2.6\times10^{-8} (300/T)^{0.44}$	8
$O^- + e \rightarrow O(^3P) + 2e$	R11	$5.74\times10^{-8} T_e^{0.324} \exp(-2.98/T_e)$	9
$O(^1D) + e \rightarrow O^+ + 2e$	R12	$9.0\times10^{-9} T_e^{0.7} \exp(-11.6/T_e)$	9
$O(^1D)(g) \xrightarrow{wall} O(^3P)$	R13	D_{eff}/Λ^2	see text
$O(^3P)(g) + O(s) \xrightarrow{wall} O_2(s) \rightarrow O_2(g)$	R14	$\gamma_{rec} D_{eff}/\Lambda^2$	see text
$O^+(g) \xrightarrow{wall} O(^3P)(g)$	R15	$2u_{B,O^+} \times (R^2 h_L + RLh_R)/R^2 L)$	see text
$O_2^+(g) \xrightarrow{wall} O_2(g)$	R16	$2u_{B,O_2^+} \times (R^2 h_L + RLh_R)/R^2 L)$	see text

Note: For R1 – R12, rate coefficient is in $cm^3\ s^{-1}$, for R13-R16 in s^{-1}, T_e in eV and T in kelvins.

The diffusion loss of metastable oxygen atoms O(1D) in Reaction 13 and atomic oxygen $O(^3P)$ in Reaction 14 to the reactor walls are estimated by an effective loss-rate coefficient[3,4] $k = \gamma_{rec} D_{eff}/\Lambda^2$, where $\Lambda^{-2} = (\pi/L)^{-2} + (2.405/R)^{-2}$ is the effective diffusion length[10,11].

$D_{eff}^{-1} = D_{AA'}^{-1} + D_{KN}^{-1}$ is the effective diffusion coefficient of the neutral species of interest, $D_{AA'} = \pi\lambda v_{th}/8$ is the neutral diffusion coefficient[6], $v_{th} = \sqrt{8k_B T/\pi M_R}$ is the mean neutral speed[8,9], $D_{KN} = v_{th}\Lambda/3$ is the free diffusion coefficient, γ_{rec} is the surface recombination coefficient for atomic oxygen on the wall surface, M_R is the reduced mass, L and R are the length and radius of the chamber, respectively. In the equation for neutral diffusion coefficient, $\lambda = (n\sigma_{AA'})^{-1}$ is the mean free path and $n = p/k_B T$. For simplicity, we assumed the neutral particles temperature of 600 K[3] to be independent on the operating parameters and cross section for collisions of oxygen atoms due to diffusion in molecular oxygen $\sigma_{AA'} \approx 3\times10^{-15}$ cm^{-2}[9]. An effective surface recombination coefficient for oxygen atoms is strongly dependent on the chamber wall materials[12]. Our chamber is composed of a combination of quartz (${\gamma_O}^{q}{}_{rec} \approx 2\times10^{-4}$)[13] and anodized Al (${\gamma_O}^{Al}{}_{rec} = 0.3$)[14]. In this work, the effective surface recombination coefficient was calculated as

$$\gamma_{rec} = ({\gamma_O}^{q}{}_{rec} * quartz\ area + {\gamma_O}^{Al}{}_{rec} * Al\ area)/total\ area \approx 4.7\times10^{-2}.$$

3. RESULTS AND DISCUSSION

Figures 1-2 show the effect of the main operating parameters on the parylene-C etch rate. From Fig. 1, it can be seen that, as the O_2 plasma input and bias power increase, the polymer etch rate increases monotonically and nearly linear in the range of 30 - 90 Å/sec. A change of the oxygen pressure does not lead to the significant changes in the etch rate (Fig. 2) and the etch rate keeps nearly constant at the range of 40 - 50 Å/sec.

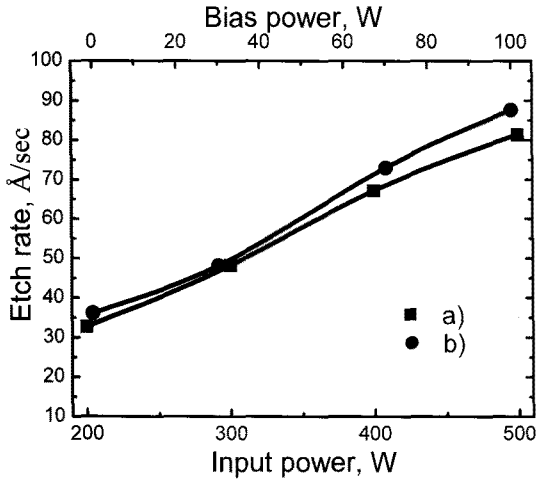

Fig. 1. Parylene-C etch rate as functions of O_2 plasma operating parameters: (a) – as functions of input power (P = 4 mTorr, W_{dc} = 30 W); (b) – as functions of bias power (P = 4 mTorr, W_{input} = 300 W).

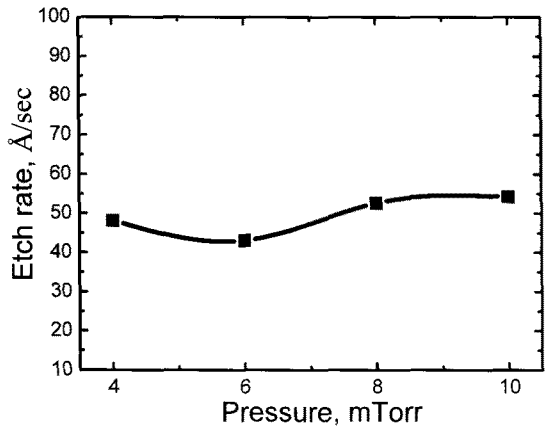

Fig. 2. Parylene-C etch rate as functions of O_2 pressure (W_{dc} = 30 W, W_{input} = 300 W).

To figure out the correlations between the behaviors of the Parylene-C etch rate and both the steady-state densities and fluxes of active species, we applied the simplified global - averaged plasma model with the Langmuir probe data on electron temperature (T_e) and total density of positive ions (n_+) as the input parameters. The calculated density of the O_2 plasma species as a function of the plasma parameters is shown in Fig. 3.

It can be easily seen that oxygen atoms in the $O(^3P)$ state is the main product of the discharge. The density of the metastable oxygen atoms and positive ions are an order of magnitude less. The increase in the input power leads to the growth of the density of the all species. As bias power and pressure increase, the behavior of active species densities doesn't demonstrate significant changes.

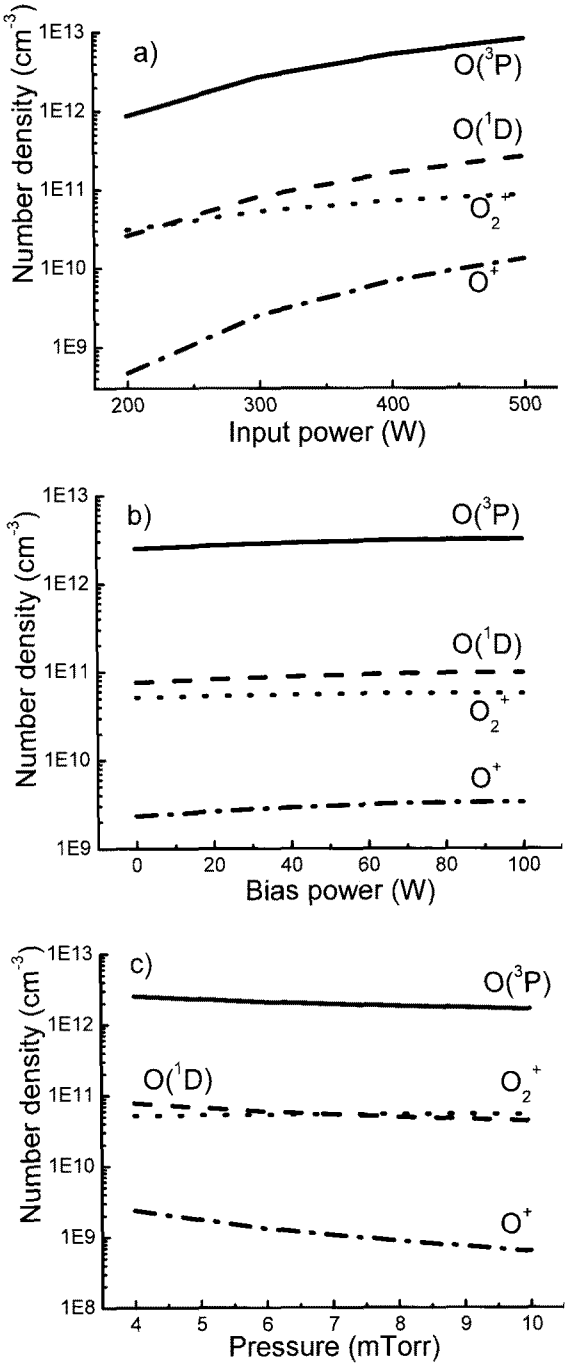

Fig. 3. Model predicted densities of neutral and charged species of O_2 discharge as functions of: a) input power (P = 4 mTorr, W_{dc} = 30 W); b) bias power (P = 4 mTorr, W_{input} = 300 W); c) pressure (W_{dc} = 30 W, W_{input} = 300 W).

However, etch rates of the materials are determined not by the volume densities, but by fluxes of active species on the surface. Over the range of plasma parameters examined, the oxygen uptake is observed and only CO_2, CO, H_2O molecules appear in the gas

phase(Fig. 4). It should be noted that the formation rates of the gaseous products due to the etching couldn't be more than fluxes of active particles.

Let's estimate the flux of the gaseous products of polymer destruction. Mass loss per time unit of the polymer is equal to the Parylene-C density $\rho \approx 1.3\,g/cm^3$ to multiply by the etch rate:

$$\Delta m \approx 1.3\,g/cm^3 \cdot (3 \div 9)\times 10^{-7}\,cm/s =$$
$$= (4 \div 12)\times 10^{-7}\,g/(cm^2 \cdot s)$$

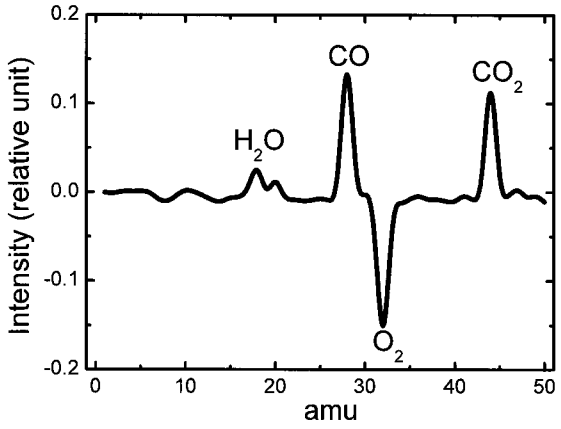

Fig. 4. Differential mass spectrum of gas phase (P = 4 mTorr, W_{input} = 300 W, W_{dc} = 30 W).

The elementary unit of the Parylene-C consists of eight carbon and hydrogen atoms and one chlorine atom, so the mass of the elementary unit $m_u \approx 2.32\times 10^{-24}\,g$. Due to the fact that main products of the ICP oxygen plasma-parylene interaction is simple molecules such as CO_2, CO, and H_2O (Fig. 4), a full flux of gaseous products from the polymer surface due to the plasma destruction is not less than the amount of atoms in the solid polymer and approximately equal to the $\Delta m/m_u \approx (2 \div 5)\times 10^{16}\,cm^{-2}\,s^{-1}$. This is the typical magnitude of the formation rate of the gaseous products in "oxidizing plasma-polymer" system.

The flux of the $O(^3P)$ atoms on the surface can be calculated from the following expression[9]:

$\Gamma_{O(^3P)} \approx \left(n_{O(^3P)}\upsilon_{th}/4\right) \sim 10^{16} \div 10^{17}\,cm^{-2}\,s^{-1}$ (see Fig. 5).

The fluxes of other species, for example the total flux of positive ions that follow to the equation[6]:

$$\Gamma_+ \approx (u_{B,(O^+)}n_{O^+} + u_{B,(O_2^+)}n_{O_2^+})\times$$
$$\times\left[(R^2h_L + RLh_R)/(R^2 + L)\right] \sim$$
$$\sim 10^{14} \div 10^{15}\,cm^{-2}\,s^{-1}$$

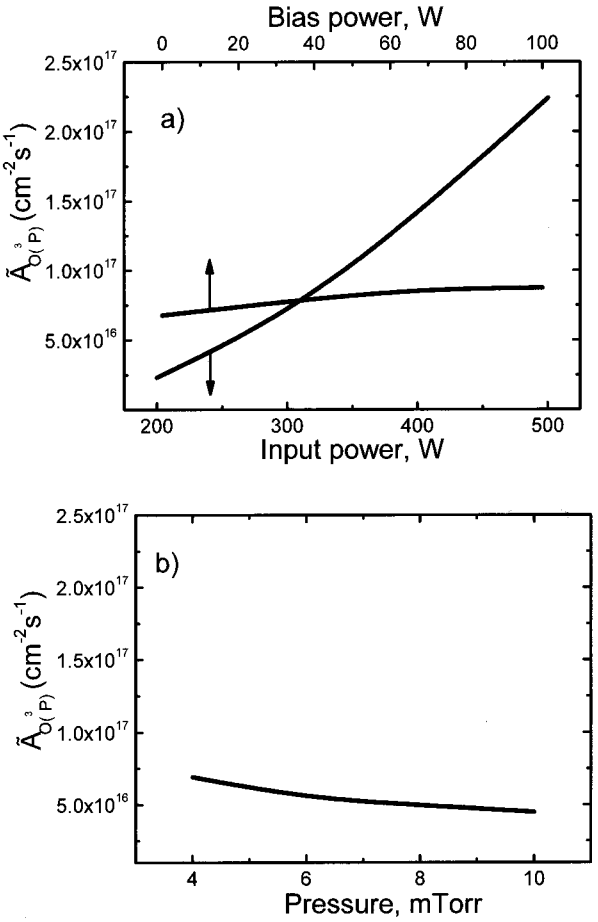

Fig. 5. Model predicted fluxes of $O(^3P)$ atoms in O_2 discharge: (a) – as functions of input power (P = 4 mTorr, W_{dc} = 30 W) and bias power (P = 4 mTorr, W_{input} = 300 W).; (b) – as functions of pressure (W_{dc} = 30 W, W_{input} = 300 W).

This equation is a few orders of magnitude below and can't provide measured etch rates of the Parylene-C. The flux behavior of oxygen atoms as a function of input power and pressure doesn't contradict to the etch rate one. At the same time, changes of the $O(^3P)$ fluxes with bias power do not describe completely observable etch rates. Obviously, it is necessary to consider the some additional factor. In our opinion, such a factor is the energy of ions. We have calculated incident ion energy for dominating O_2^+ ion as $\varepsilon \approx e\left(0.5T_e + U_f + U_{dc}\right)$- the sum of ion acceleration energy in the plasma sheath and the negative dc bias voltage, which is applied to the substrate. Ion energy as a function of discharge condition is shown in Fig. 6. As input power increase, the incident energy of ions shows a weak reduction tendency. At the same time, the increase in the bias power leads to the sharp growth of the negative dc bias voltage and also the increase in the ion incident energy. A change of oxygen

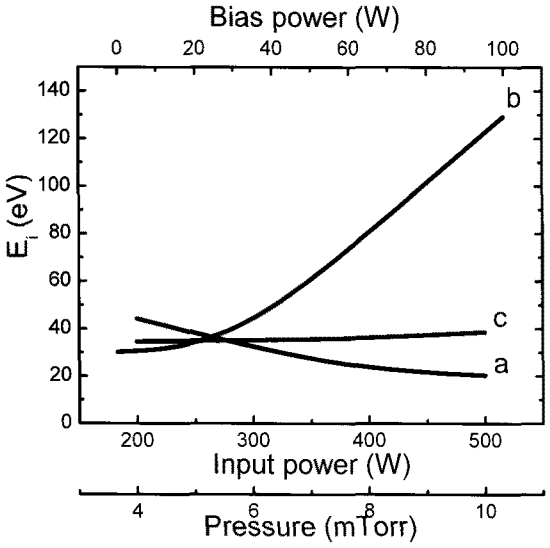

Fig. 6. Calculated incident ion energy: (a) – as functions of input power (P = 4 mTorr, W_{dc} = 30 W); (b) – as functions of bias power (P = 4 mTorr, W_{input} = 300 W); (c) – as functions of pressure (W_{dc} = 30 W, W_{input} = 300 W).

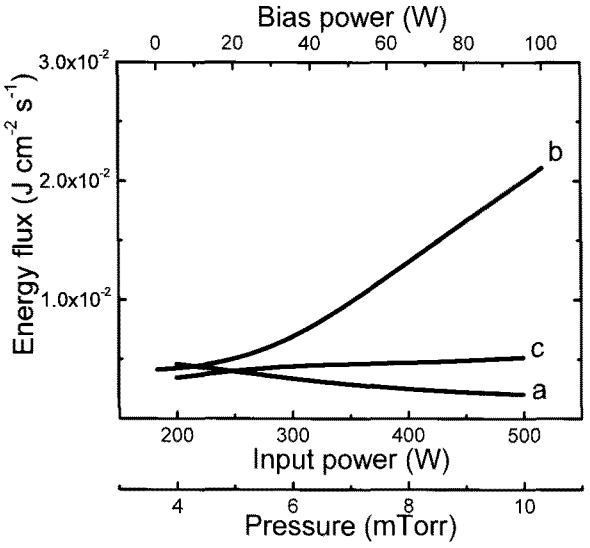

Fig. 7. Calculated energy fluxes: (a) – as functions of input power (P = 4 mTorr, W_{dc} = 30 W); (b) – as functions of bias power (P = 4 mTorr, W_{input} = 300 W); (c) – as functions of pressure (W_{dc} = 30 W, W_{input} = 300 W).

pressure does not lead to significant changes in the incident ion energy. We have estimated total energy flux transferred from plasma to the polymer surface by ions as the product of ion energy and ion flux(Fig. 7). It can be seen that fluxes of oxygen atoms stay nearly constant with increasing the bias power, whereas incident ion energy sharply increases. So, in our opinion, ions do not directly participate in polymer etching. The basic role of ions is energy transfer to macromolecules of the polymer. Energy dissipation on the polymer surface results in the excitation of macromolecules, bond's breaking, and the formation of surface radicals. The increase in the transmitted energy from plasma to polymer due to ion bombardment increases the concentration of the intermediate active centers at polymer surfaces.

Hence the increase in the chemical interaction's probability of atomic oxygen with polymer is appropriate. It explains "etch rate-bias power" regularity.

4. CONCLUSION

Etch rates of the Parylene-C in the inductively coupled O_2 plasma in the wide range of the discharge parameters were investigated. By analysis of the effect of process parameters on etch rates with calculated plasma species concentrations and fluxes, we can conclude that the main etching agent of the Parylene-C is oxygen atoms $O(^3P)$. At the same time, it can be assumed that positive ions are effective channel of energy transfer from plasma towards polymer and the formation of surface radicals.

ACKNOWLEDGEMENTS

This work was supported by the Korea Research Foundation Grant funded by the Korean Government (MOEHRD) (KRF-2007-313-D00292).

REFERENCES

[1] C. D. Dimitrakopoulos, B. K. Furman, T. Graham, S. Hegde, and S. Purushothaman, "Field-effect transistors comprising molecular beam deposited α,ω-di-hexyl-hexathienylene and polymeric insulator", Synth. Met., Vol. 92, p. 47, 1998.

[2] K. N. Narayanan Unni, S. Dabos-Seignon, and J.-M. Nunzi, "Influence of the polymer dielectric characteristics on the performance of a quaterthiophene organic field-effect transistor", J. Mater. Sci., Vol. 41, p. 1865, 2006.

[3] C. Lee, D. B. Graves, M. A. Lieberman, and D. W. Hess, "Global model of plasma chemistry in a high density oxygen discharge", J. Electrochem. Soc., Vol. 141, p. 1547, 1994.

[4] C. Lee and M. A. Lieberman, "Global model of Ar, O_2, Cl_2, and Ar/O_2 high-density plasma discharges", J. Vac. Sci. Technol. A, Vol. 13, p. 368, 1995.

[5] J. T. Gudmundsson and M. A. Lieberman, "Model and measurements for a planar inductive oxygen discharge", Plasma Sources. Sci. Technol., Vol. 7,

p. 1, 1998.
[6] J. T. Gudmundsson, A. M. Marakhtanov, K. K. Patel, V. P. Gopinath, and M. A. Lieberman, "On the plasma parameters of a planar inductive oxygen discharge", J. Phys. D: Appl. Phys., Vol. 33, p. 1323, 2000.
[7] J. T. Gudmundsson, I. G. Kouznetsov, K. K. Patel, and M. A. Lieberman, "Electronegativity of low-pressure high-density oxygen discharges", J. Phys. D: Appl. Phys., Vol. 34, p. 1100, 2001.
[8] S. Kim, M. A. Lieberman, A. J. Lichtenberg and J. T. Gudmundsson, "Improved volume-averaged model for steady and pulsed-power electronegative discharges", J. Vac. Sci. Technol. A, Vol. 24, p. 2025, 2006.
[9] M. A. Lieberman and A. J. Lichtenberg, "Principles of plasma discharges and materials processing", John Wiley & Sons Inc., New York, 2004.
[10] P. J. Chantry, "A simple formula for diffusion calculations involving wall reflection and low density", J. Appl. Phys., Vol. 62, p. 1141,1987.
[11] V. Phelps, "The diffusion of charged particles in collisional plasmas. Free and ambipolar diffusion at low and moderate pressures", J. Res. Natl. Inst. Stand. Technol., Vol. 95, p. 407, 1990.
[12] S. Gomez, P. G. Steen, and W. G. Graham, "Atomic oxygen surface loss coefficient measurements in a capacitive/inductive radio-frequency plasma", Appl. Phys. Lett., Vol. 81, p. 19, 2002.
[13] J. C. Greaves and J. W. Linnett, "Recombination of atoms at surfaces. Part 6.- Recombination of oxygen atoms on silica from 20 °C to 600 °C", Trans. Faraday Soc., Vol. 55, p. 1355, 1959.
[14] P. F. Kurunczi, J. Guha, and V. M. Donnelly, "Recombination reactions of oxygen atoms on an anodized aluminum plasma reactor wall, studied by a spinning wall method", J. Phys. Chem. B, Vol. 109, p. 20989, 2005.